NASA TM- 81876

NASA Technical Memorandum 81876

INTERLAMINAR STRESS SINGULARITIES AT A STRAIGHT FREE EDGE IN COMPOSITE LAMINATES

I. S. Raju and John H. Crews, Jr.

FOR REFERENCE

August 1980

F

NASA

National Aeronautics and
Space Administration

Langley Research Center
Hampton, Virginia 23665
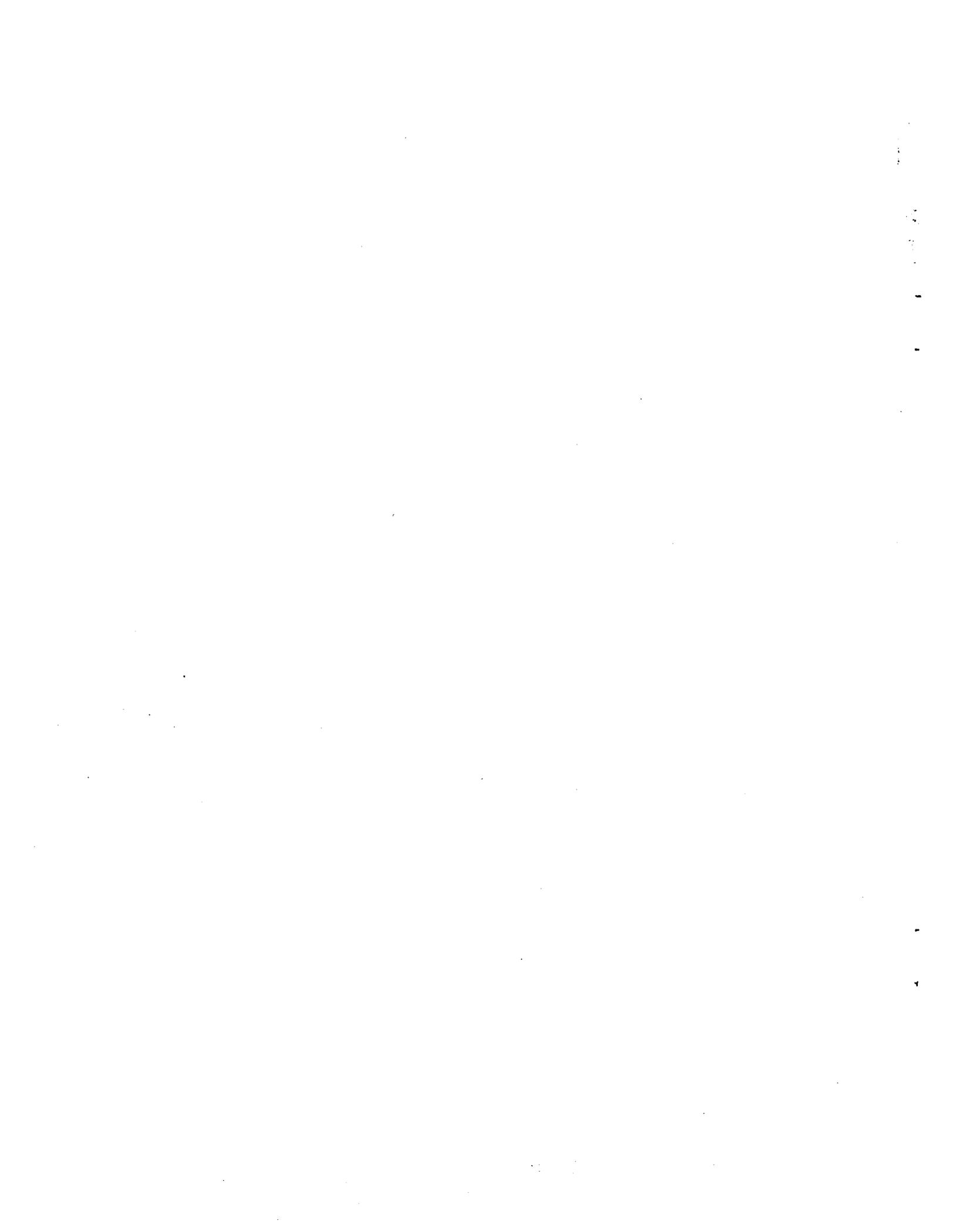
INTERLAMINAR STRESS SINGULARITIES AT A STRAIGHT

FREE EDGE IN COMPOSITE LAMINATES

I. S. Raju[*] and John H. Crews, Jr.
NASA Langley Research Center
Hampton, Virginia 23665

SUMMARY

A quasi-three-dimensional finite-element analysis was used to analyze the edge-stress problem in four-ply, composite laminates. The seven laminates that were considered belong to the laminate family $[\theta/(\theta-90)]_s$, where $0 \leq \theta \leq 90$. Systematic convergence studies were made to explore the existence of stress singularities near the free edge. The present analysis appears to confirm the existence of stress singularities at the intersection of the interface and the free edge. The power of the stress singularity was the same for all seven laminates considered.

INTRODUCTION

Many composite laminates develop high interlaminar stresses near free edges due to mechanical loads, thermal loads, or hygroscopic effects. The interlaminar stresses can lead to delamination and eventual failure of the laminate. Several numerical analyses have computed stress distributions in a finite-width laminate subjected to uniform axial strain. This case is often referred to as the straight-edge or the edge-stress problem. In reference 1, a finite-difference scheme was used to analyze the edge-stress problem of a $[\pm 45]_s$ laminate. In reference 2, a three-dimensional finite-element method was used to analyze the edge effects in $[\pm 45]_s$ and $[90/0]_s$ laminates. In reference 3, a

quasi-three-dimensional finite-element analysis was used to analyze $[0/90]_s$, $[90/0]_s$, $[\pm45]_s$, and several quasi-isotropic laminates. These analyses used coarse mesh models because of limitations on computing storages and times. However, all showed that the interlaminar stresses had very localized peaks near the free edge. If these localized peaks were caused by a singularity, as suggested in references 1 and 3, singularity analyses could be developed and used to study delaminations.

The present study investigated the existence of stress singularities at a free edge in several four-ply laminates that belong to the laminate family $[\theta/(\theta-90)]_s$, $0 \leq \theta \leq 90$. To this end, quasi-three-dimensional finite-element analysis was used. The analysis, which is similar to that of reference 3, used eight-noded isoparametric elements.

The interlaminar stresses are presented as distributions through the thickness at the free edge, and along the interface between the plies. The results are compared and discussed for seven different laminates. Stress distributions calculated from the analyses were used in a procedure to investigate the existence of stress singularities.

SYMBOLS

A_1 strength of singularity, MPa

b   half-width of the straight-edge laminate, m

E_{ii} Young's modulus in i-direction, MPa

G_{ij} shear modulus, MPa

h   ply thickness, m

r   nondimensional distance from the free edge, $r = (b - y)/h$

U,V,W   displacement functions, m

u,v,w   displacements in x-, y-, and z-directions, respectively, m

x,y,z   Cartesian coordinates, m

α power of the singularity

ϵ_o uniform axial strain imposed on the straight-edge laminate, $\epsilon_o = 0.001$

θ outer ply angle, deg

ν_{ij} Poisson's ratios

$\{\sigma\}$ Cartesian stresses, σ_x, σ_y, σ_z, σ_{xy}, σ_{yz}, σ_{zx}, MPa

Subscripts:

i,j $i,j = 1,2,3$

1,2,3   longitudinal, transverse, and thickness directions of a unidirectional ply

ANALYSIS

This section describes the laminates analyzed, the quasi-three-dimensional formulation, and the finite-element idealizations used in this study. This section also discusses the procedure used to investigate the existence of a stress singularity.

Laminates

The laminates considered in the analyses were $[0/90]_s$, $[15/-75]_s$, $[30/-60]_s$, $[\pm 45]_s$, $[60/-30]_s$, $[75/-15]_s$, and $[90/0]_s$. As previously mentioned, these seven laminates belong to the family $[\theta/(\theta-90)]_s$, $0 \leq \theta \leq 90$. The top ply angle, θ, is shown in figure 1(a).

Each ply was idealized as a homogeneous, elastic orthotropic material with properties (refs. 1, 2, and 3),

$$E_{11} = 137.9 \text{ GPa } (20 \times 10^6 \text{ psi})$$

$$E_{22} = E_{33} = 14.48 \text{ GPa } (2.1 \times 10^6 \text{ psi})$$

$$G_{12} = G_{23} = G_{31} = 5.86 \text{ GPa } (0.85 \times 10^6 \text{ psi})$$

$$\nu_{12} = \nu_{13} = \nu_{23} = 0.21$$

The subscripts 1, 2, and 3 correspond to the longitudinal, transverse, and thickness directions, respectively, of the individual ply.

Quasi-Three-Dimensional Analysis

Figure 1(a) shows a long, symmetric laminate loaded in the x-direction. The laminate has a width of 2b and has four plies, each of thickness h. Away from the ends, the displacements in any x = constant plane were assumed to be

$$
\left.
\begin{aligned}
u(x,y,z) &= \epsilon_o x + U(y,z) \\
v(x,y,z) &= V(y,z) \\
w(x,y,z) &= W(y,z)
\end{aligned}
\right\} \tag{1}
$$

where ϵ_o is a uniform axial strain, and U,V,W are functions of the coordinates y and z alone (ref. 1). Furthermore, because of symmetries inherent in the layups considered, U, V, and W satisfy the following requirements:

$$
\left.
\begin{aligned}
U(y,z) &= -U(-y,-z) \\
V(y,z) &= -V(-y,z) \\
W(y,z) &= -W(y,-z)
\end{aligned}
\right\} \tag{2}
$$

and

$$\frac{\partial}{\partial z} U(y,0) = \frac{\partial}{\partial z} V(y,0) = \frac{\partial}{\partial y} W(0,z) = 0$$

The displacement field of equations (1) should satisfy the equations of equilibrium and the stress-free conditions on the edges, $y = \pm b$, and top and bottom surfaces, $z = \pm 2h$.

Because exact solutions are not available for the complex three-dimensional problem, approximate methods were used in references 1 through 3. The present study was based on a finite-element analysis, like that in reference 3, except eight-noded quadrilateral isoparametric elements were used rather than three-noded triangular elements.

Finite-Element Idealizations

Because of the symmetries in the problem, only one quadrant of an x = constant plane was idealized. The quadrant ($0 \leq y \leq b$ and $0 \leq z \leq 2h$) is shown as the shaded region in figure 1(b). The displacement functions U and V were prescribed as zero on the $y = 0$ line, and the displacement function W was prescribed as zero on the $z = 0$ line.

The shaded region in figure 1(b) was idealized by eight-noded isoparametric elements in the rectangular-mesh models shown in figure 2 and the polar-mesh model in figure 3. The rectangular-mesh model had a rectangular arrangement throughout. In contrast, the polar model had a polar mesh near the free edge and rectangular arrangement elsewhere. The rectangular mesh was used to compute the stress distributions, and the polar mesh was used to investigate the stress singularities.

To study the convergence of the stresses near the free edge, three rectangular meshes were used. The medium mesh in figure 2(b) was obtained by

subdividing each element of the coarse mesh (fig. 2(a)) into four elements.
Similarly, the fine mesh in figure 2(c) was obtained by subdividing each ele-
ment of the medium mesh into four elements. The coarse mesh had 135 nodes and
36 elements, the medium mesh had 485 nodes and 144 elements, and the fine mesh
had 1833 nodes and 576 elements.

The polar mesh had the polar arrangement in the region ($19h \leq y \leq 20h$,
$0 \leq z \leq 2h$) near the laminate free edge. As in the rectangular-mesh case,
three meshes--coarse, medium, and fine--were used. Only the polar fine mesh
is shown in figure 3. The three polar meshes had the same number of nodes and
elements as their corresponding rectangular counterparts. Near the free edge,
however, the polar fine mesh was an order of magnitude finer than the rectangu-
lar fine mesh.

Analysis of Singularities

The stress distribution along a radial line from a singularity can be
expressed as (refs. 4 and 5)

$$\sigma = A_1 r^{-\alpha} + 0\left(r^{-\alpha+1}\right) \tag{3}$$

where r is the distance from the singularity, A_1 and α are constants,
and $0\left(r^{-\alpha+1}\right)$ represents terms of the order $r^{-\alpha+1}$ and higher. For small
distances r, the singular term dominates and equation (3) can be approxi-
mated by

$$\sigma \simeq A_1 r^{-\alpha}$$

or

$$\log \sigma = \log A_1 - \alpha \log r \tag{4}$$

Hence, a log σ vs. log r plot would be a line with a slope of -α and a σ-intercept of A_1. The α and A_1 are the power and the strength of the singularity, respectively.

Equation (4) provided the basis for a precedure to investigate the existence of stress singularities at the laminate edge. This equation was fitted to the computed stresses. If the equation fitted these stresses well and if the slope of the fitted line was negative, a stress singularity with power α was indicated. This log-linear procedure was verified in reference 4 by applying it to several well-known singular-stress problems in two-dimensional elasticity.

The log-linear procedure works best where the singular term strongly dominates the other terms. Therefore, the procedure should be applied only in the regions very close to the singularity.

RESULTS AND DISCUSSION

First, distributions are presented for interlaminar normal stress σ_z and the shear stress σ_{xz} for the various $[\theta/(\theta-90)]_s$, $0 \leq \theta \leq 90$, laminates. Then, the results are investigated for the existence of stress singularities at the free edge. For convenience, the intersection of the interface and the free edge (z = h; y = b) will be called the interface corner. Similarly, the intersection of the midplane and the free edge (z = 0; y = b) will be called the midplane corner.

The uniform axial strain, ε_o, was arbitrarily set equal to 0.001 throughout this study.

Stress Distributions

The stresses with the steepest gradients near the free edge were the normal stress σ_z and the shear stress σ_{xz}. The distributions for these

stresses, through the thickness and along the interface, are presented and compared in this section.

Interlaminar normal stress, σ_z.—

[0/90]$_s$ laminate: Figure 4(a) shows the σ_z distribution through the thickness along the free edge (y = b) for the three rectangular meshes (coarse, medium, and fine). In this figure and all subsequent figures, the fine mesh results are represented by a curve through the data; only the value at the interface is shown as a discrete value (diamond symbol). The coarse and medium mesh results are shown by circular and square symbols, respectively. The solid symbols indicate the stresses in the top ply. As shown on the figure, the values of σ_z for the three meshes agree closely except near the interface (z = h). At the interface the three meshes produced noticeably different values. In addition, σ_z is discontinuous across the interface; this discontinuity is slightly larger with progressive mesh refinement. Hence, the stress state shown in figure 4(a) suggests that a singularity exists at the interface corner. In contrast, at the midplane (z = o) the σ_z values agree for the three meshes and show no evidence of a singularity at the midplane corner.

Figure 4(b) shows the average σ_z from both plies plotted against a normalized distance from the edge. The σ_z results from the three meshes are in excellent agreement for (b - y)/h > 0.08. However, at the free edge, y = b, the computed σ_z values are noticeably different for the three meshes, with the fine mesh producing the largest value. Therefore, results in both figures 4(a) and 4(b) suggest that a singularity exists at the interface corner.

[±45]$_s$ laminate: Figure 5(a) shows the σ_z distribution through the thickness at the free edge (y = b). As in the [0/90]$_s$ laminate, the values of σ_z for the three meshes agree closely everywhere except near the interface (z = h), where a steep gradient exists. Figure 5(b) shows the distribution of

σ_z along the interface. As expected, the results from the three meshes agree except very near the free edge. Further, the computed value of σ_z at the free edge was larger for progressive mesh refinement. These results for the $[\pm 45]_s$ laminate also suggest a σ_z singularity at the interface corner.

Other laminates: Figures 6 and 7 show the σ_z distributions through the thickness and along the interface for $[15/-75]_s$, $[75/-15]_s$, $[30/-60]_s$, and $[60/-30]_s$, respectively. In these figures only the fine mesh results are shown. The distributions of σ_z near the free edge have steep gradients for all the four laminates, indicating a possible singularity.

Comparisons: The results in figures 4 through 7 show that, except for $[0/90]_s$ and $[90/0]_s$ laminates, the interlaminar normal stress, σ_z, is compressive at the interface corner. In contrast, at the midplane corner only laminates $[75/-15]_s$ and $[90/0]_s$ develop compressive σ_z.

Interlaminar shear stress, σ_{xz}. -

$[\pm 45]_s$ laminate: Figure 8(a) presents the through-the-thickness distributions of σ_{xz} at the free edge obtained using the three rectangular meshes for the $[\pm 45]_s$ laminate. Figure 8(b) shows the σ_{xz} distribution along the interface. For all the meshes σ_{xz} closely agrees everywhere except near the interface in figure 8(a) and free edge in figure 8(b). The gradients are steep in this region, again indicating a possible singularity for the $[\pm 45]_s$ laminate.

Other laminates: For the other laminates considered the σ_{xz} distributions were similar to the $[\pm 45]_s$ results and, therefore, are not shown. Also, the average σ_{xz} values at the interface for a laminate and its corresponding complementary laminate $\left(\text{for example, } [15/-75]_s \text{ and } [75/-15]_s\right)$ differed only in the third significant digit.

Comparisons: For all laminates considered the σ_{xz} distributions had the same sign along the interface. The $[15/-75]_s$ and $[75/-15]_s$ developed the largest σ_{xz} very near the free edge compared to other laminates. Near the free edge, the σ_{xz} stresses are larger (by at least a factor of 3) than the corresponding σ_z stresses in each laminate, except for the $[0/90]_s$ and $[90/0]_s$ laminates for which σ_{xz} is identically zero.

For all laminates considered, σ_{xz} is identically zero at the midplane because of symmetry. Therefore, analysis of singularities is confined to the neighborhood of the interface corner.

Singularities

Both the σ_z and σ_{xz} distributions suggest that singularities exist at the interface corner. To identify these singularities, both σ_z and σ_{xz} stress data may be used in the log-linear procedure outlined in the analysis section. However, for the present edge-stress case (generalized plane strain), if one stress is singular at a point, then all stresses are and they all have the same singularity power, α. This conclusion follows from the observation that these stresses have similar functional forms, derived from the same order derivatives of the same stress functions, as shown in reference 6. Therefore, either σ_z or σ_{xz} may be used in the log-linear procedure to determine the power of the singularity.

To decide which stress was better suited for the log-linear procedure, known singularities were examined. The case of a center-cracked plate showed that the log-linear procedure gave best results when the predominant stress was used. For the present study, the σ_{xz} stress was predominant. As previously mentioned, the σ_{xz} values near the edge were at least three times as large as the σ_z values, except for the $[0/90]_s$ and $[90/0]_s$ laminates. Further, as

pointed out earlier, the procedure works best when the singular term in equation (3) strongly dominates the other terms. The σ_{xz} distributions had the same sign all along the interface; in contrast, the σ_z distributions changed sign near the edge. This suggests that the singular term for σ_{xz} is dominant over a wider range of data than for σ_z. For these reasons σ_{xz} was used in the log-linear procedure.

The results for the rectangular and polar meshes were indistinguishable for distances greater than 0.04h from the free edge. Very near the free edge, however, the polar mesh yielded a greater concentration of data and, therefore, was used to analyze stress singularities.

$[\pm 45]_s$ laminate.- Figure 9 shows the log-log plots of the absolute value of σ_{xz}, along the interface for a $[\pm 45]_s$ laminate, plotted against r. The stresses obtained from the three polar meshes are plotted in this figure. As expected, all three meshes show a linear portion with a negative slope, indicating a singularity. Before calculating the power of the singularity, the linear region for each set of data was estimated visually. (The two points closest to the edge were neglected because they represent nodes for the element at the singularity, and this element cannot be expected to yield accurate stresses.) Stresses from the coarse, medium, and fine meshes appear to be linear in the ranges of $0.0125 \leq r \leq 0.07$, $0.0035 \leq r \leq 0.015$, and $0.0015 \leq r \leq 0.01$, respectively. In these ranges a linear least-square-fitting procedure was used to determine the power (α) and the strength (A_1) of the singularity in the equation

$$\log \sigma_{xz} = \log A_1 - \alpha \log r$$

The following values were found for the three meshes.

	POLAR MESH		
	COARSE	MEDIUM	FINE
Mesh index, i	1	2	3
Power, α	0.256	0.182	0.170
Percent change in α, $\dfrac{\alpha_i - \alpha_{i+1}}{\alpha_i}$ (100)	-	41	7
Strength A_1, MPa	5.702	7.509	7.950

As shown in the table, by refining the coarse mesh to generate the medium mesh, the α changed by 41 percent. For the fine mesh, the additional refinement produced only a 7-percent change, which is only about one-sixth the 42-percent change. Further mesh refinement (dividing each fine mesh element into four elements) would probably cause an additional 1-percent change (one-sixth of 7 percent). This 1-percent change is neglibibly small. Similar arguments can be made for the strength of the singularity, A_1. Therefore, the present fine mesh results were treated as converged values.

To check the accuracy of the present procedure, the $[\pm 45]_s$ singularity was computed using the σ_{xz} stresses along nine different radial lines of the polar mesh. The calculated power of the singularity α should be the same for all such lines. Figure 10 shows α and the corresponding A_1 values plotted against ϕ, the angular position of each radial line. These values of α vary slightly, from 0.195 at $\phi = 0$ to an interface value of 0.170 at $\phi = \pi/2$. At the interface, the σ_{xz} stresses were largest, as shown by the

largest A_1 value at $\phi = \pi/2$ in figure 10. As mentioned earlier, the present procedure yields best results when the predominant stresses are used. Because the σ_{xz} stress was largest at the interface ($\phi = \pi/2$), the α value of 0.170 is believed to be accurate. Also, the absolute value of the correlation coefficient in the least-square procedure was closest to unity (0.9996) for $\phi = \pi/2$.

Other laminates.- The σ_{xz} stress was also used to identify the singularities for the $[15/-75]_s$, $[75/-15]_s$, $[30/-60]_s$, and $[60/-30]_s$ laminates. Figure 11 shows the log-log plots for these four laminates. For comparison the previous results for the $[\pm 45]_s$ laminate are also included in this figure.

As pointed out earlier, for a laminate and its complementary laminate the σ_{xz} results differed only in the third significant digit. Therefore, the power of the singularity for a laminate and its complement is apparently identical. Also note that log-linear plots in figure 11 are parallel to each other. Therefore, the power of the singularities for $[15/-75]_s$, $[75/-15]_s$, $[30/-60]_s$, and $[60/-30]_s$ are identical to that for the $[\pm 45]_s$ case, that is, 0.170. However, the three parallel lines in figure 11 are separated, indicating different singularity strengths, A_1.

Figure 12 shows α and A_1 for various $[\theta/(\theta-90)]_s$ laminates as functions of the outer ply angle, θ. To investigate α and A_1 in the region $0 \leq \theta \leq 15$ (and $75 \leq \theta \leq 90$), the laminates $[2/-88]_s$ and $[7.5/-82.5]_s$ were also considered. The α values for these laminates are nearly equal to 0.170, but the A_1 values are much smaller than for the other laminates. This was expected because the σ_{xz} stress is identically zero for $[0/90]_s$ and $[90/0]_s$ laminates; thus, for θ nearly equal to zero A_1 should also be very small. Dotted lines in figure 12 represent extrapolations to zero.

Figure 12 shows that both α and A_1 are symmetric about $\theta = 45°$. Also, the strength, A_1, is maximum for the $[15/-75]_s$ and $[75/-15]_s$ laminates.

$[0/90]_s$ and $[90/0]_s$ laminates.- For the $[0/90]_s$ laminate, σ_z was used in the log-linear procedure because the σ_{xz} was identically zero. As expected, the log-log plot in figure 13 shows a linear region with a negative slope. The power of the singularity was obtained from the least-square procedure as 0.202. This power is larger than the 0.17 calculated from other laminates but is only slightly beyond the range shown in figure 10. The computed power of 0.202 probably occurred because the σ_z singularity for the $[0/90]_s$ laminate was not as dominant as the σ_{xz} singularity analyzed for the other laminates. However, if the log-linear procedure were applied to σ_z stresses for smaller r values, the power may also approach 0.17. Such calculations for smaller r values would require further mesh refinement, which is beyond the scope of this paper.

For the $[90/0]_s$ laminate neither σ_z nor σ_{xz} could be used in the log-linear procedure. The σ_{xz} was identically zero and the σ_z changed sign very near the free edge (see fig. 4(b)). Consequently, the singularity for the $[90/0]_s$ laminate was not computed. However, as shown previously for other laminates, a laminate and its complementary laminate have the same α. Therefore, by induction, the singularities for $[0/90]_s$ and $[90/0]_s$ should also be identical and α should be 0.17.

In general, these results suggest that the power of the singularities for $[\theta/(\theta-90)]_s$, $0 \le \theta \le 90$, laminates with material properties used in this paper is about 0.17. This power should be interpreted only as an approximate value because of the numerical accuracy of the log-linear procedure.

CONCLUDING REMARKS

The stresses near a straight, free edge in composite laminates subjected to uniform axial strain were studied by a quasi-three-dimensional finite-element analysis. Seven different four-ply laminates were analyzed: $[0/90]_s$, $[15/-75]_s$, $[30/-60]_s$, $[\pm 45]_s$, $[60/-30]_s$, $[75/-15]_s$, and $[90/0]_s$—belonging to the family $[\theta/(\theta-90)]_s$, $0 \le \theta \le 90$. The laminates were idealized by eight-noded isoparametric elements. Systematic convergence studies were made with the aid of three meshes to examine the interlaminar stresses near the free edge.

Near the intersection of the interface and the free edge, the interlaminar normal stress σ_z was tensile for $[0/90]_s$ and $[90/0]_s$ laminates and was compressive for all other laminates considered. The interlaminar shear stress σ_{xz} was much larger than the normal stress σ_z for all laminates except for $[0/90]_s$ and $[90/0]_s$ laminates (for which σ_{xz} is identically zero). Among the laminates considered, laminates $[15/-75]_s$ and $[75/-15]_s$ developed the highest σ_{xz}.

Convergence studies indicated that stress singularities probably exist at the intersection of the interface and the free edge, and the singularities do not exist at the midplane. A log-linear curve fitting procedure appears to confirm the existence of a singular point at the intersection of the interface and free edge. The shear stress data close to the singular point were used in the log-linear procedure to evaluate the power of the singularities.

The present results suggest that the power of the singularity is the same for all orthotropic laminates in the family represented by $[\theta/(\theta-90)]_s$, $0 \le \theta \le 90$ for a given set of material properties. For these laminates, with material properties of the graphite/epoxy considered, the power of the singularity was about 0.17.

REFERENCES

1. R. B. Pipes and N. J. Pagano, Interlaminar stresses in composite laminates under uniform axial extension. J. Comp. Materials 4, 538-548 (1970).

2. E. F. Rybicki, Approximate three-dimensional solutions for symmetric laminates under in-plane loading. J. Comp. Materials 5, 354-360 (1971).

3. A. S. D. Wang and F. W. Crossman, Some new results on edge effect in symmetric composite laminates. J. Comp. Materials 11, 92-106 (1977).

4. E. B. Becker, R. S. Dunham, and M. Stern, Some stress intensity calculations using finite elements. Proceedings of the 1974 International Conference on Finite Element Methods in Engineering (Edited by V. A. Pulmans and A. P. Kabaila, 117-138 (1974).

5. M. L. Williams, Stress singularities resulting from various boundary conditions in angular corners of plates in extension. J. Appl. Mech. 19, 526-528 (1952).

6. S. G. Lekhnitskii, Theory of Elasticity of an Anisotropic Elastic Body. Holden-Day, Inc., San Francisco (1963).
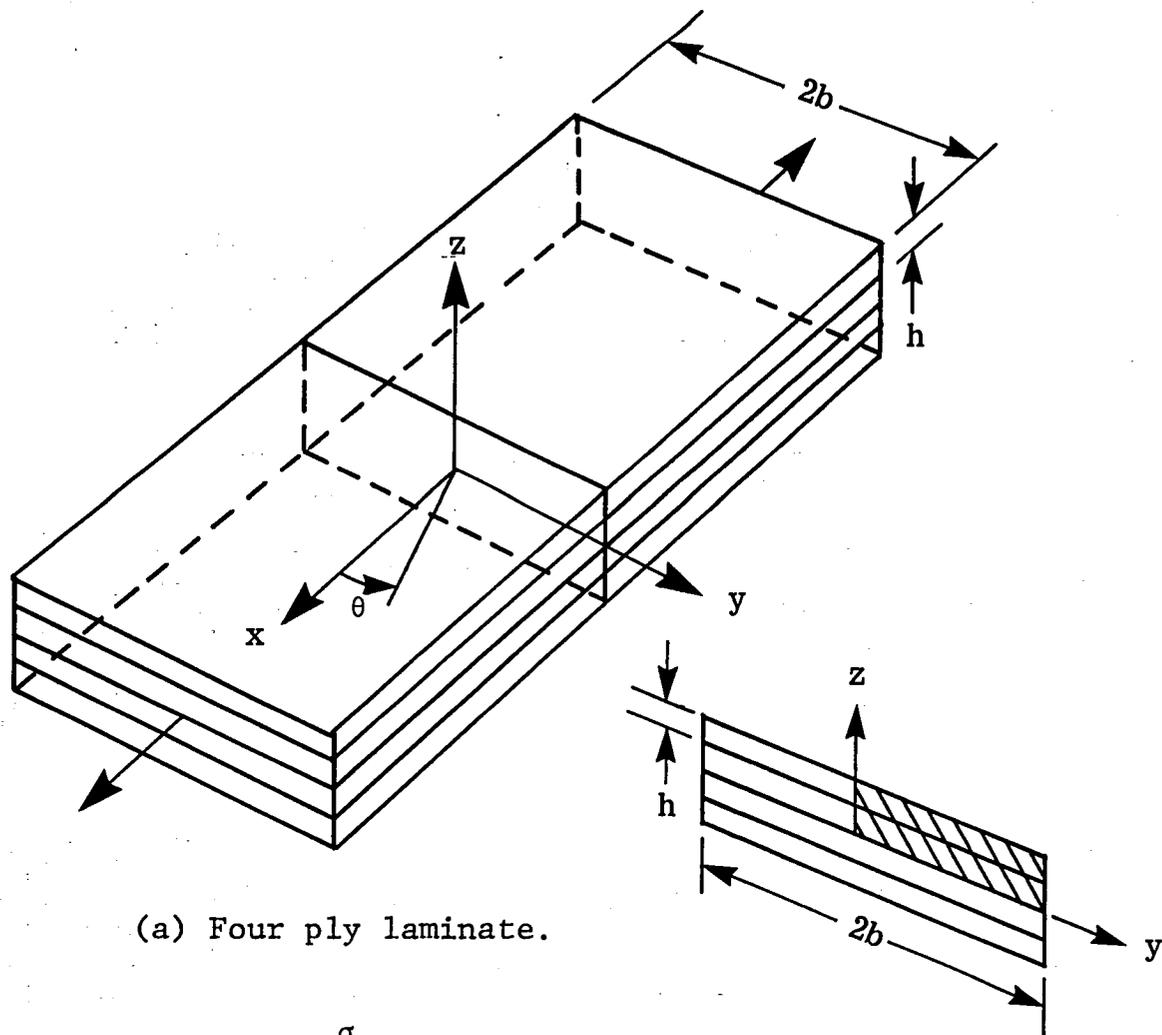
(a) Four ply laminate.

(b) An x = constant plane.
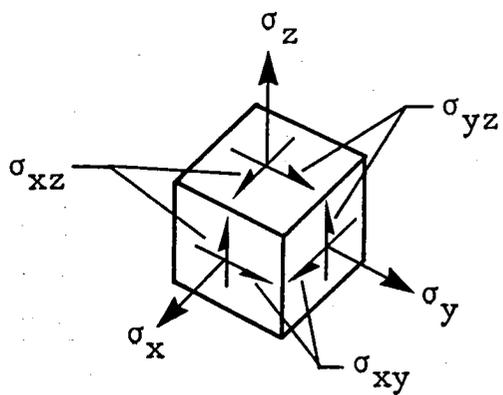
(c) 3-D stress components.

Figure 1.- Laminate configuration, loading, and stresses.
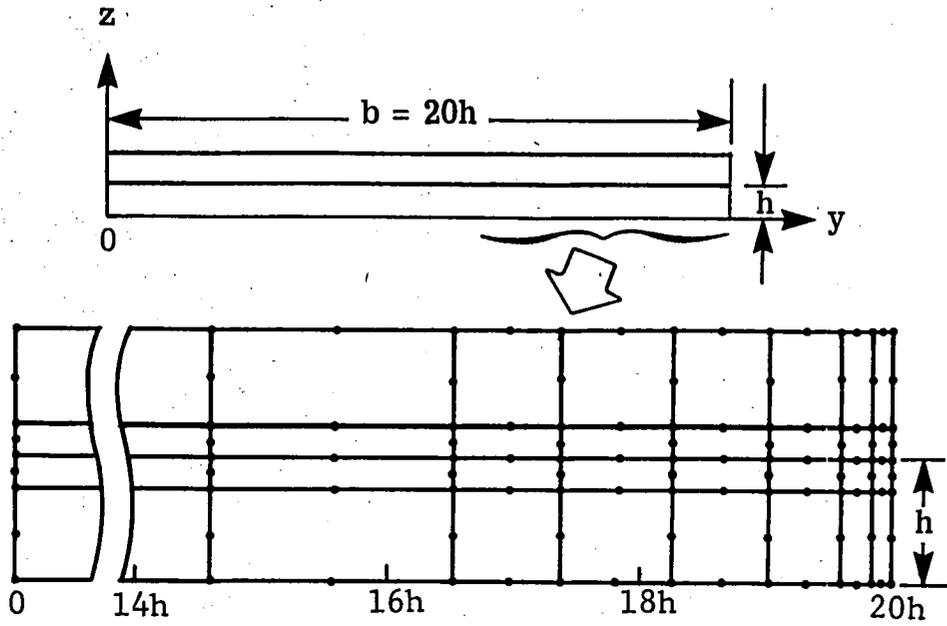
(a) Coarse mesh.
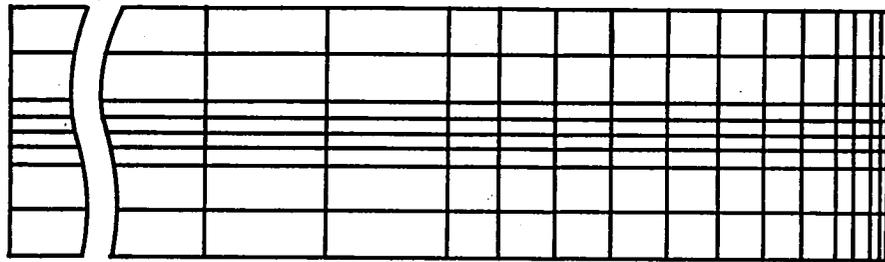
(b) Medium mesh.
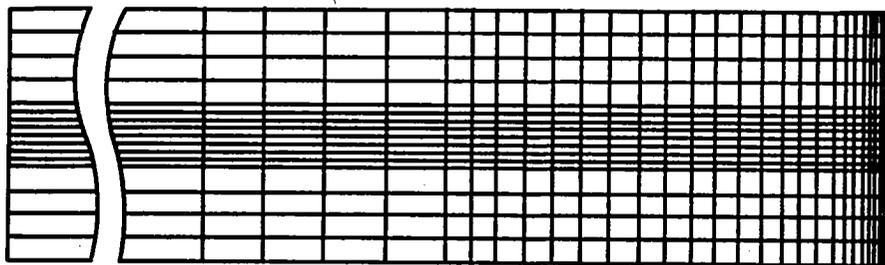
(c) Fine mesh.

Figure 2.- Rectangular mesh models.
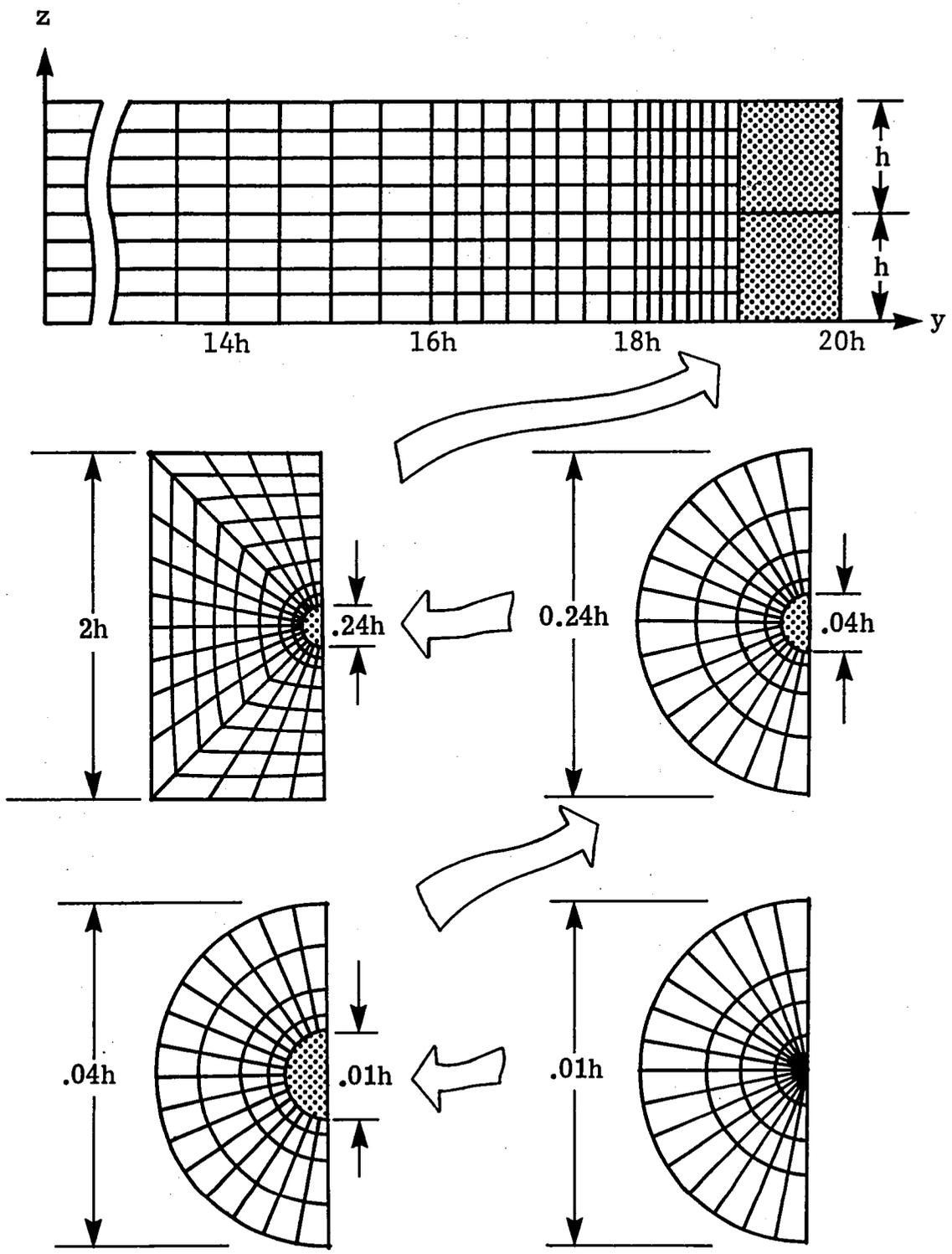
Figure 3.- Fine polar mesh model.
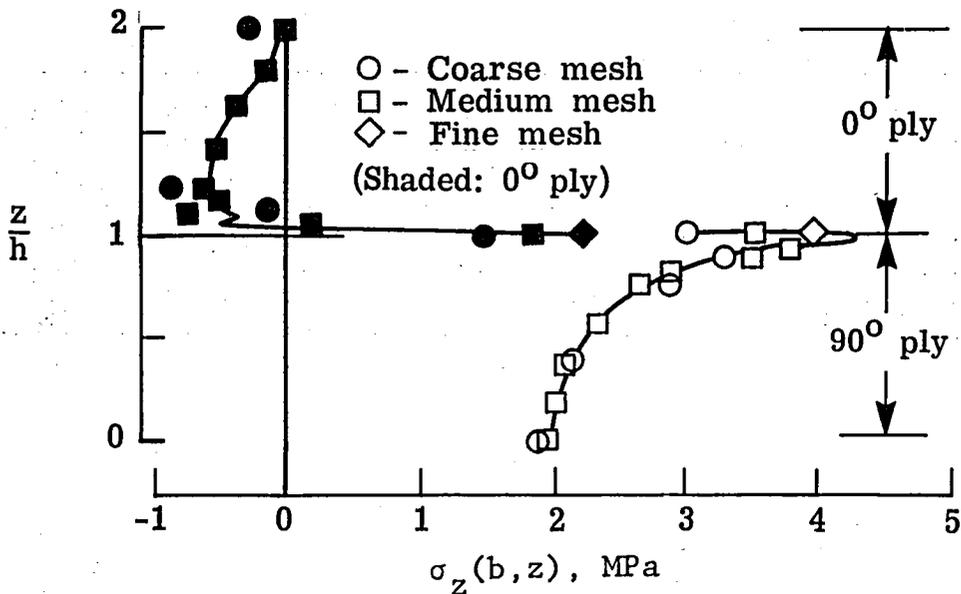
(a) σ_z along the free edge, $y = b$.
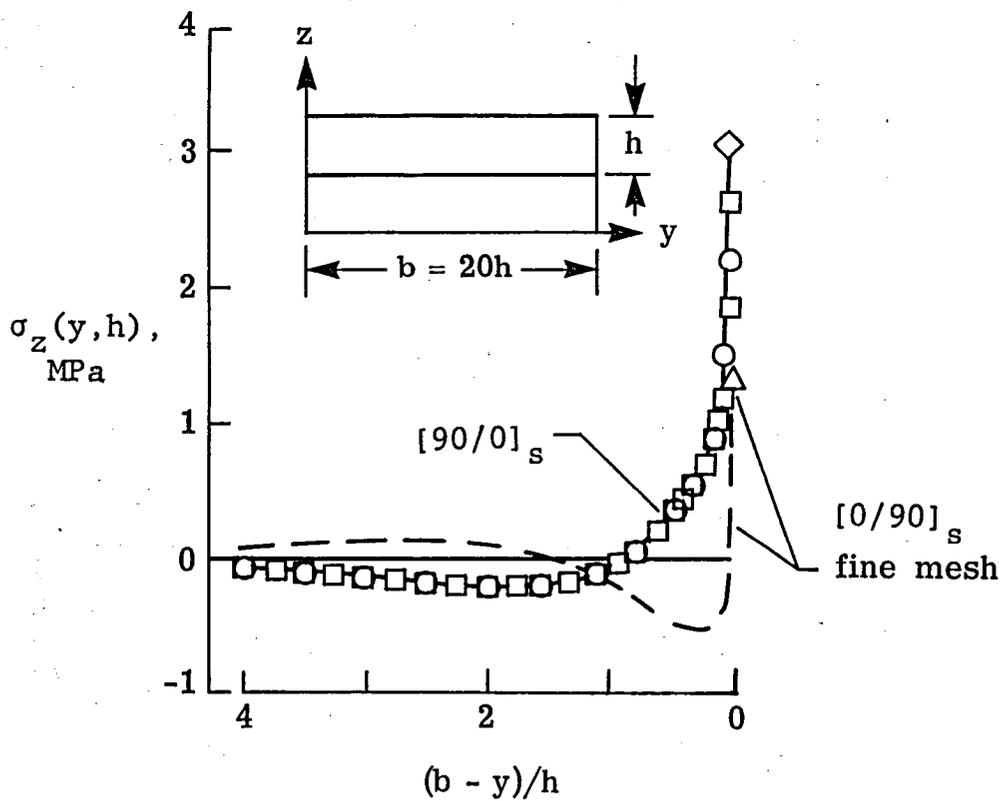
(b) σ_z along the interface, $z = h$.

Figure 4.- The σ_z distributions for $[0/90]_s$ and $[90/0]_s$ laminates.
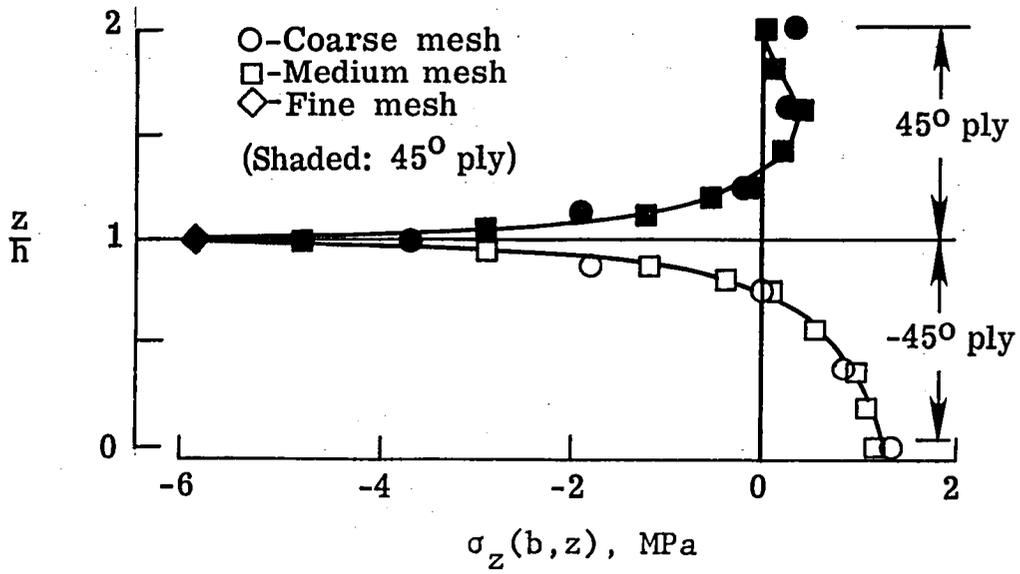
(a) σ_z along the free edge, $y = b$.
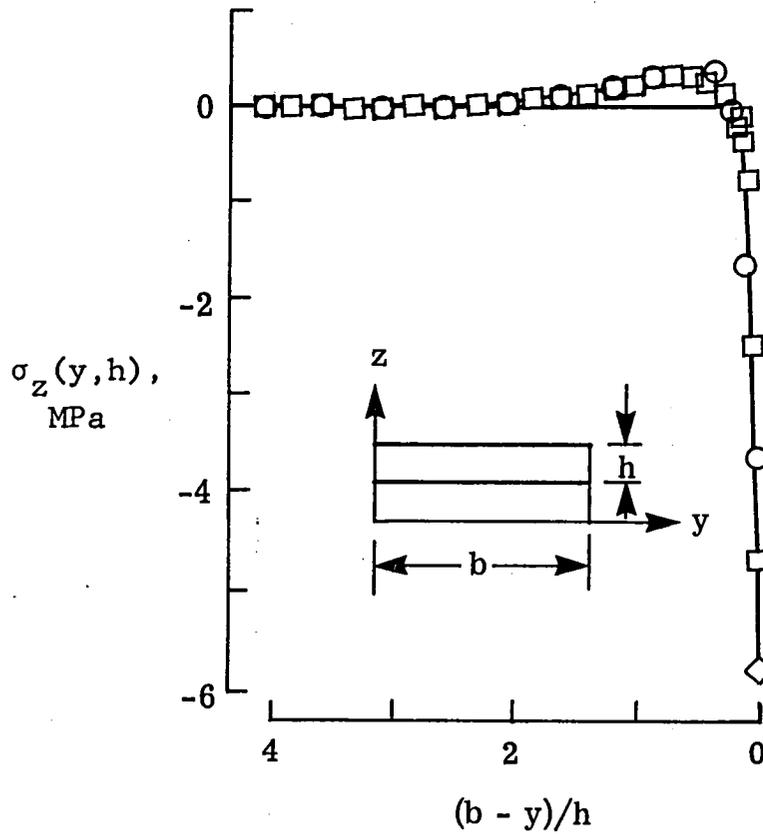
(b) σ_z along the interface, $z = h$.

Figure 5.- The σ_z distributions for $[\pm 45]_s$ laminate.

22
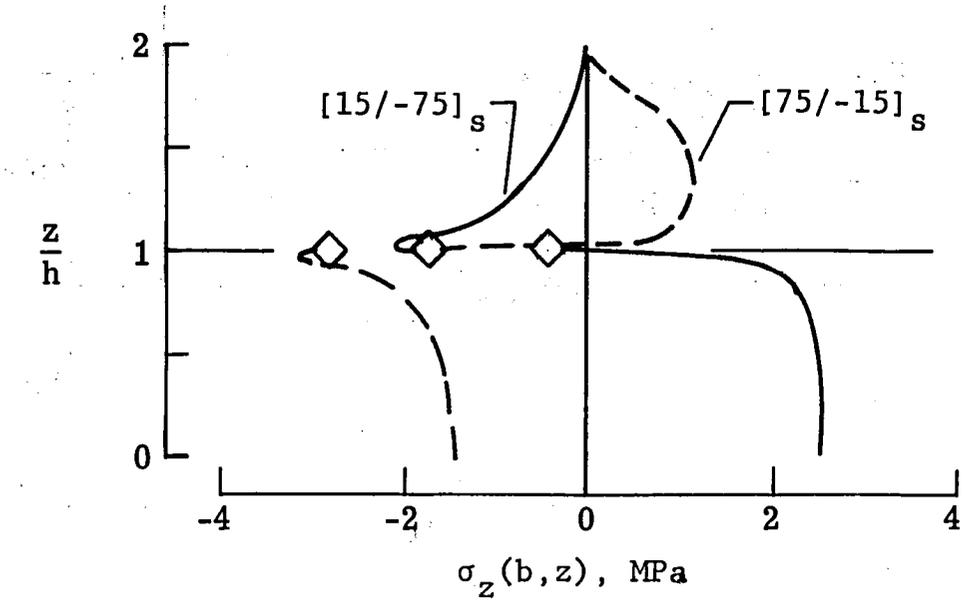
(a) σ_z along the free edge, y = b.
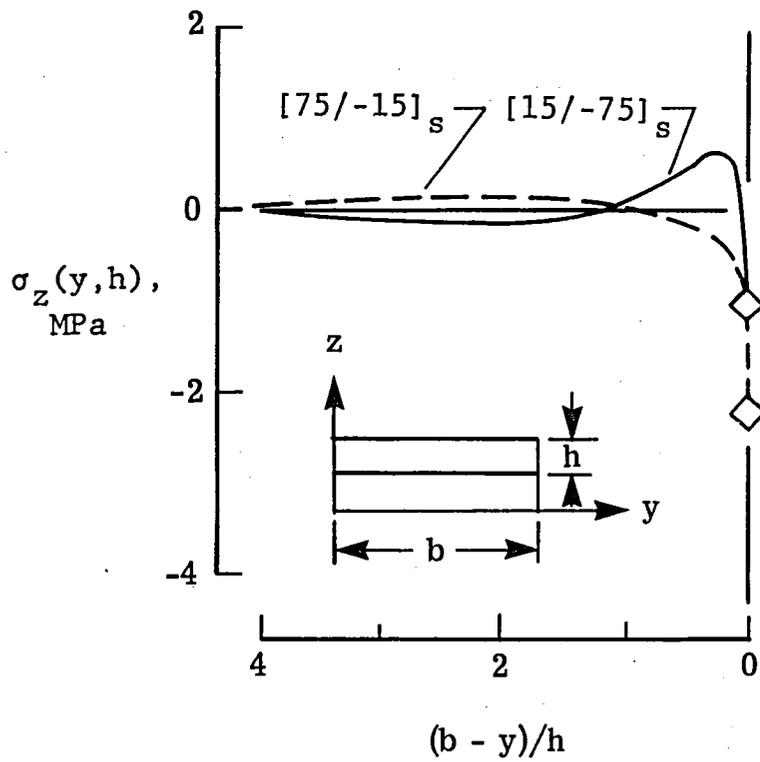
(b) σ_z along the interface, z = h.

Figure 6.- The σ_z distributions for $[15/-75]_s$ and $[75/-15]_s$ laminates, fine mesh.

(a) σ_z along the free edge, $y = b$.

(b) σ_z along the interface, $z = h$.
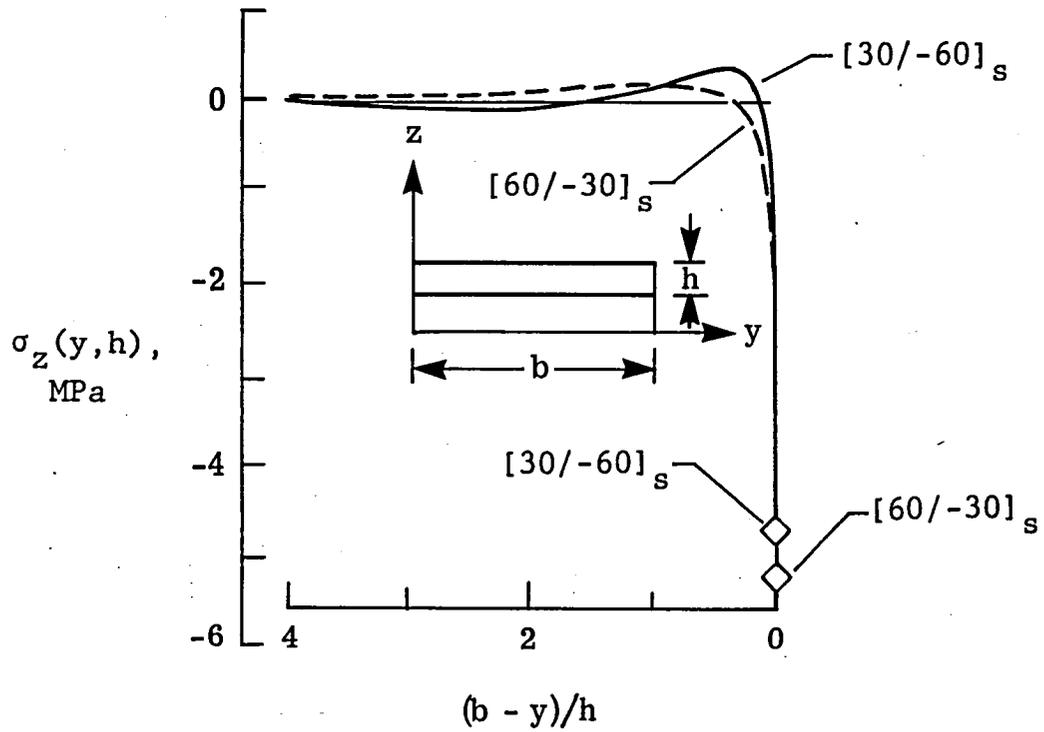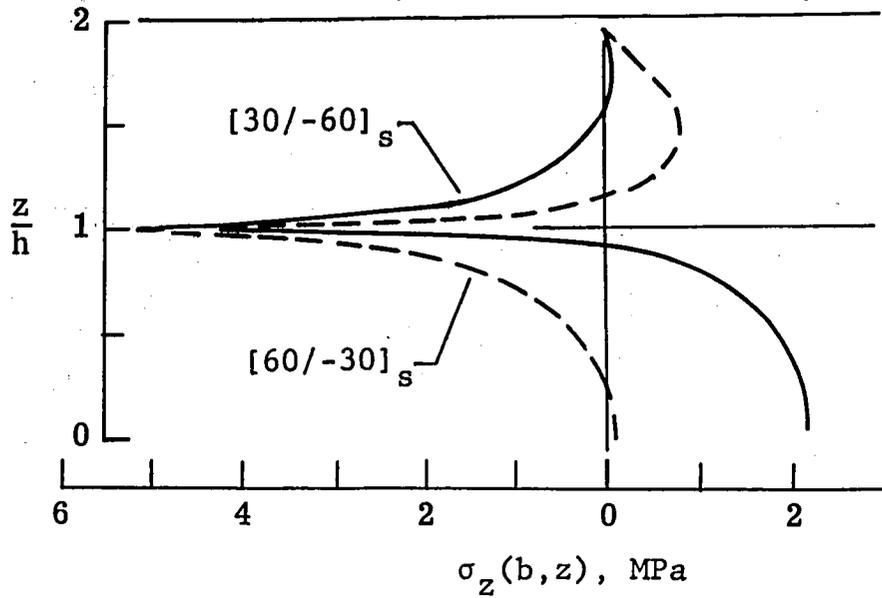
Figure 7.- The σ_z distributions for $[30/-60]_s$ and $[60/-30]_s$ laminates, fine mesh.
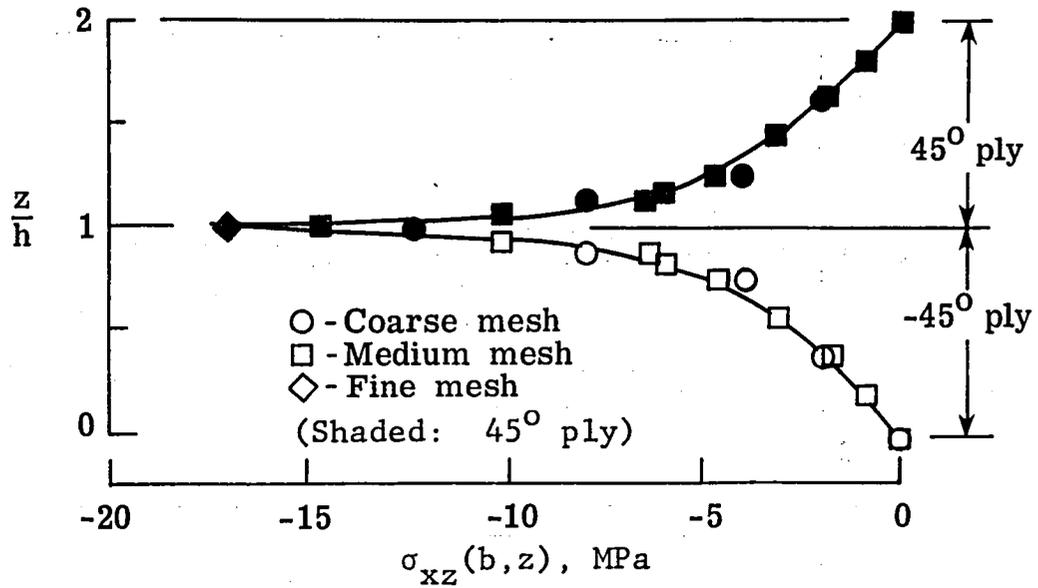
(a) σ_{xz} along the free edge, y = b.
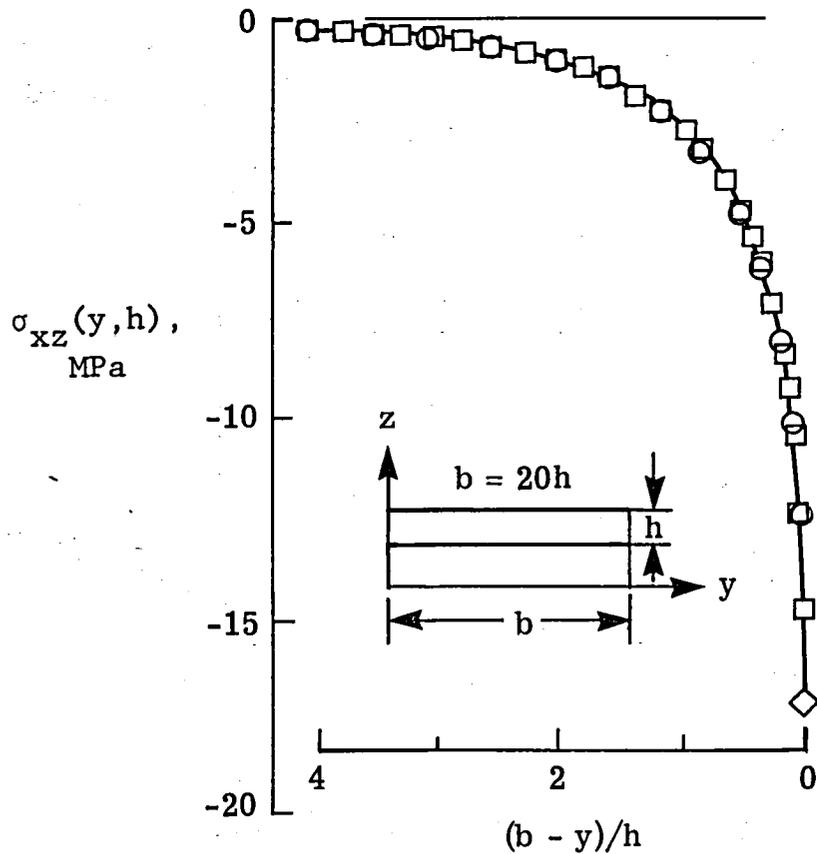
(b) σ_{xz} along the interface, z = h.

Figure 8.- The σ_{xz} distributions for the $[\pm 45]_s$ laminate.
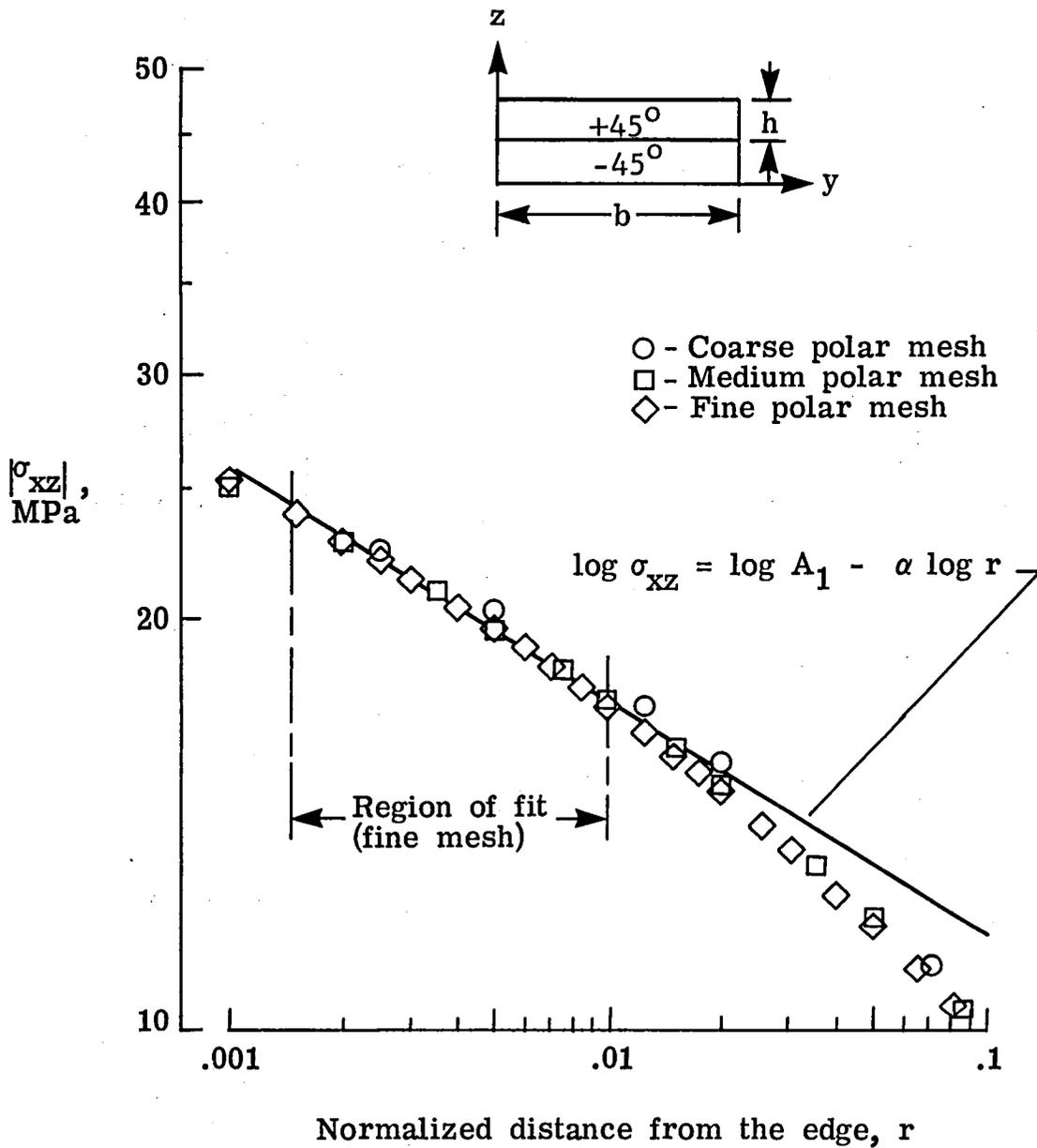
Figure 9.- Log-log plot for σ_{xz} along the interface $(z = h)$ for the $[\pm 45]_s$ laminate.
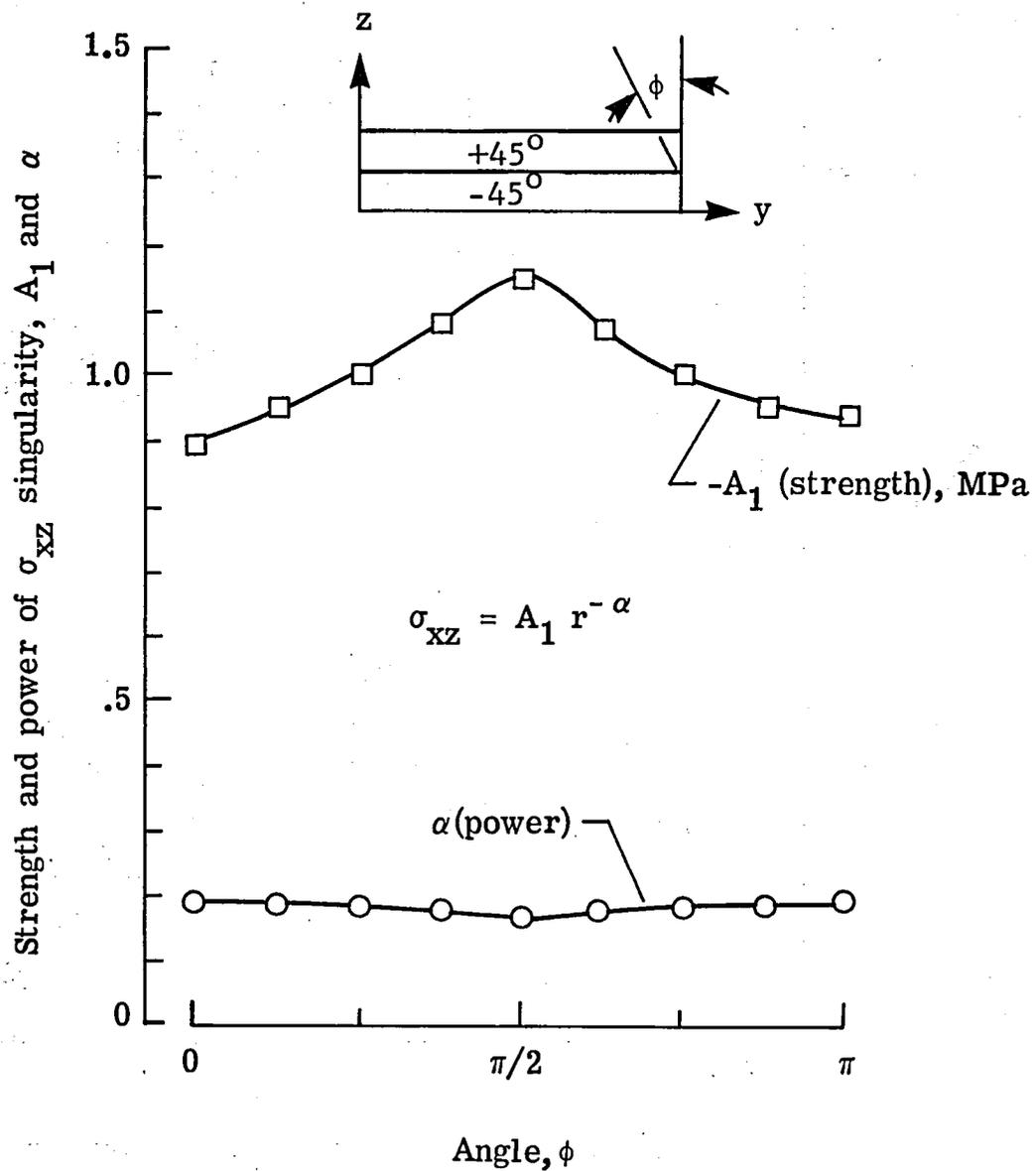
Figure 10.- Angular variation of strength and power of σ_{xz} singularity for $[\pm 45]_s$ laminate.
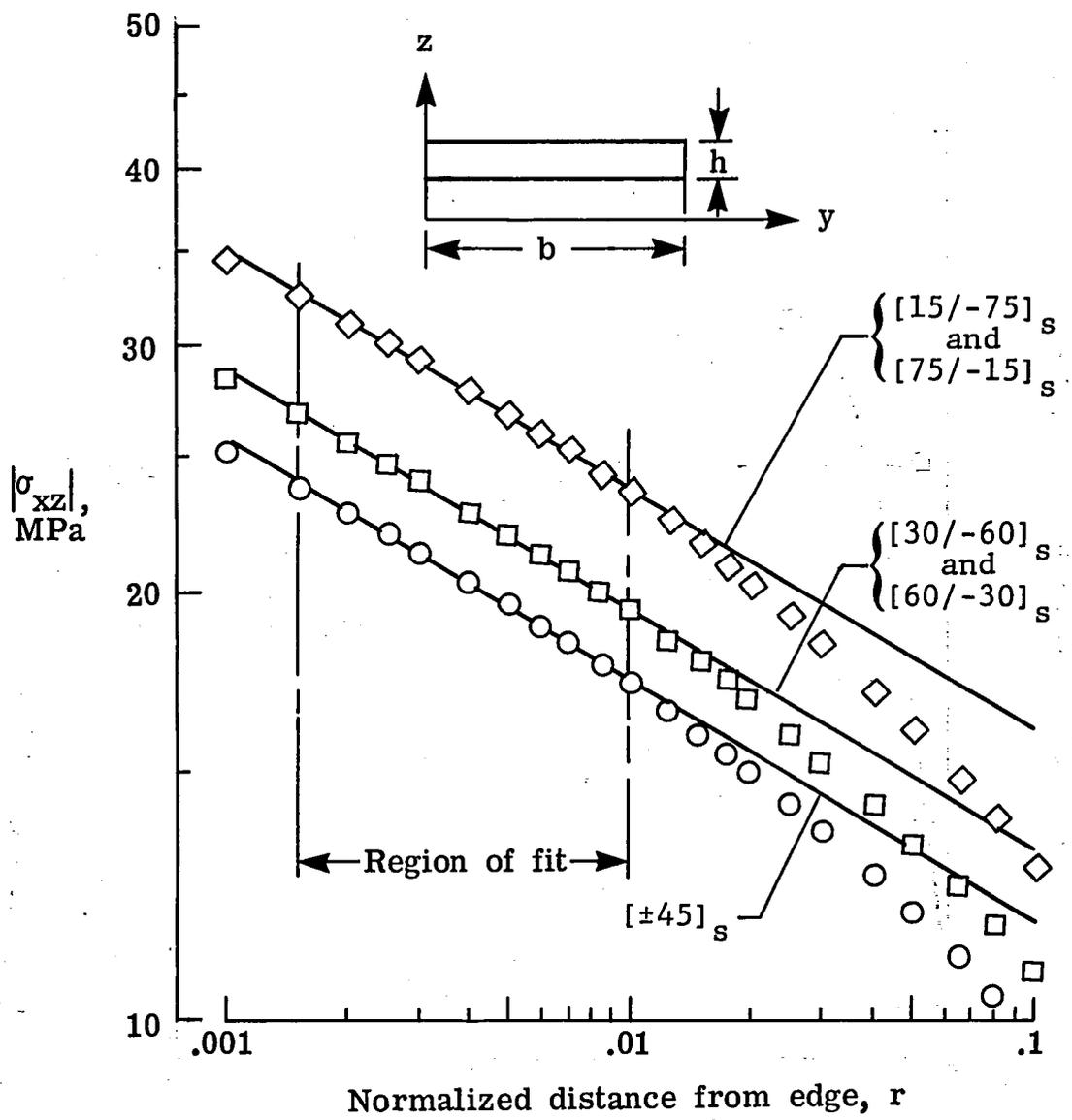
Figure 11.- Log-log plot for σ_{xz} along interface (z = h) for various laminates.
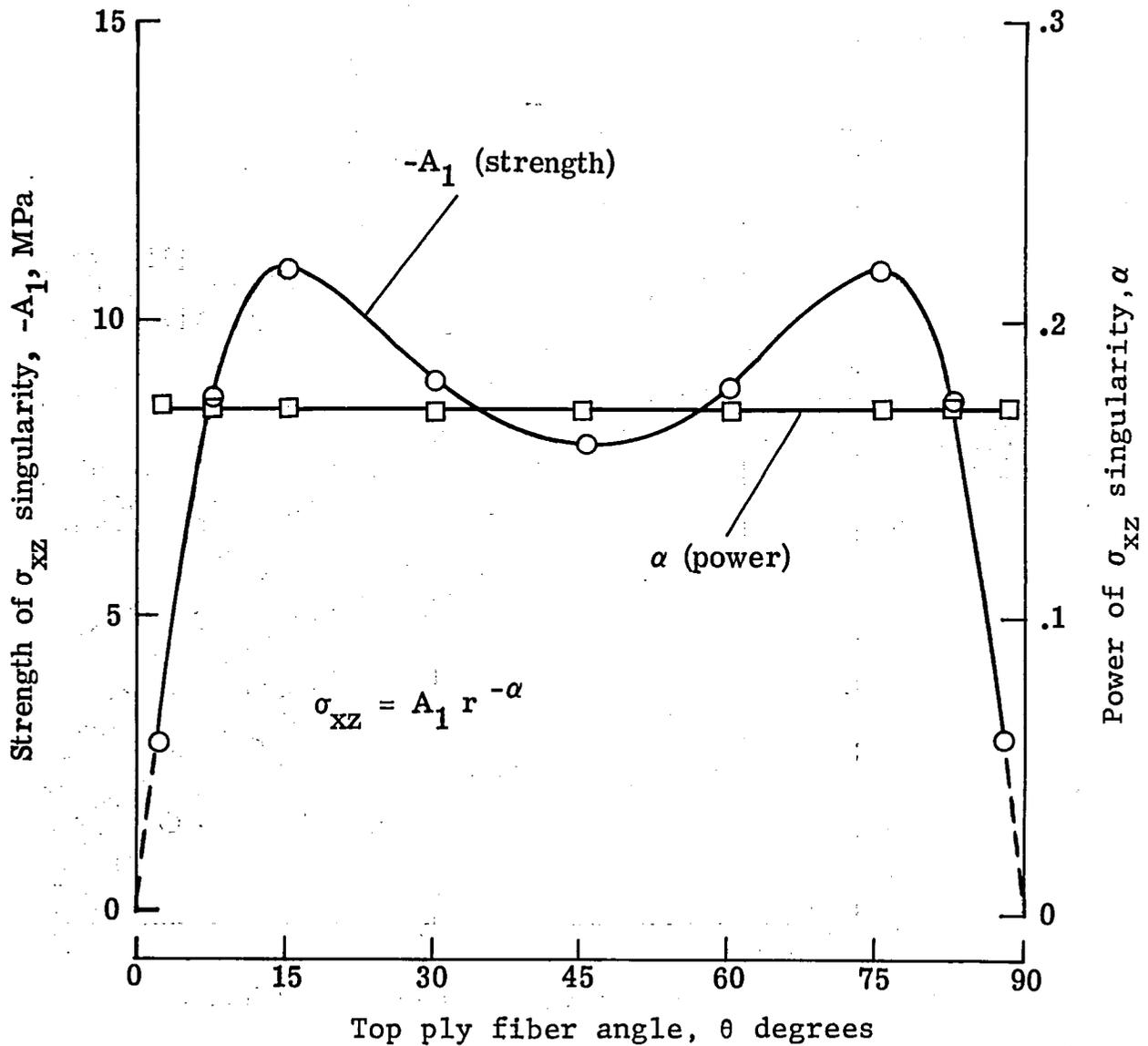
Figure 12.- Strength and power of σ_{xz} singularity for $[\theta/(\theta-90)]_s$, $0 \le \theta \le 90$, laminates.
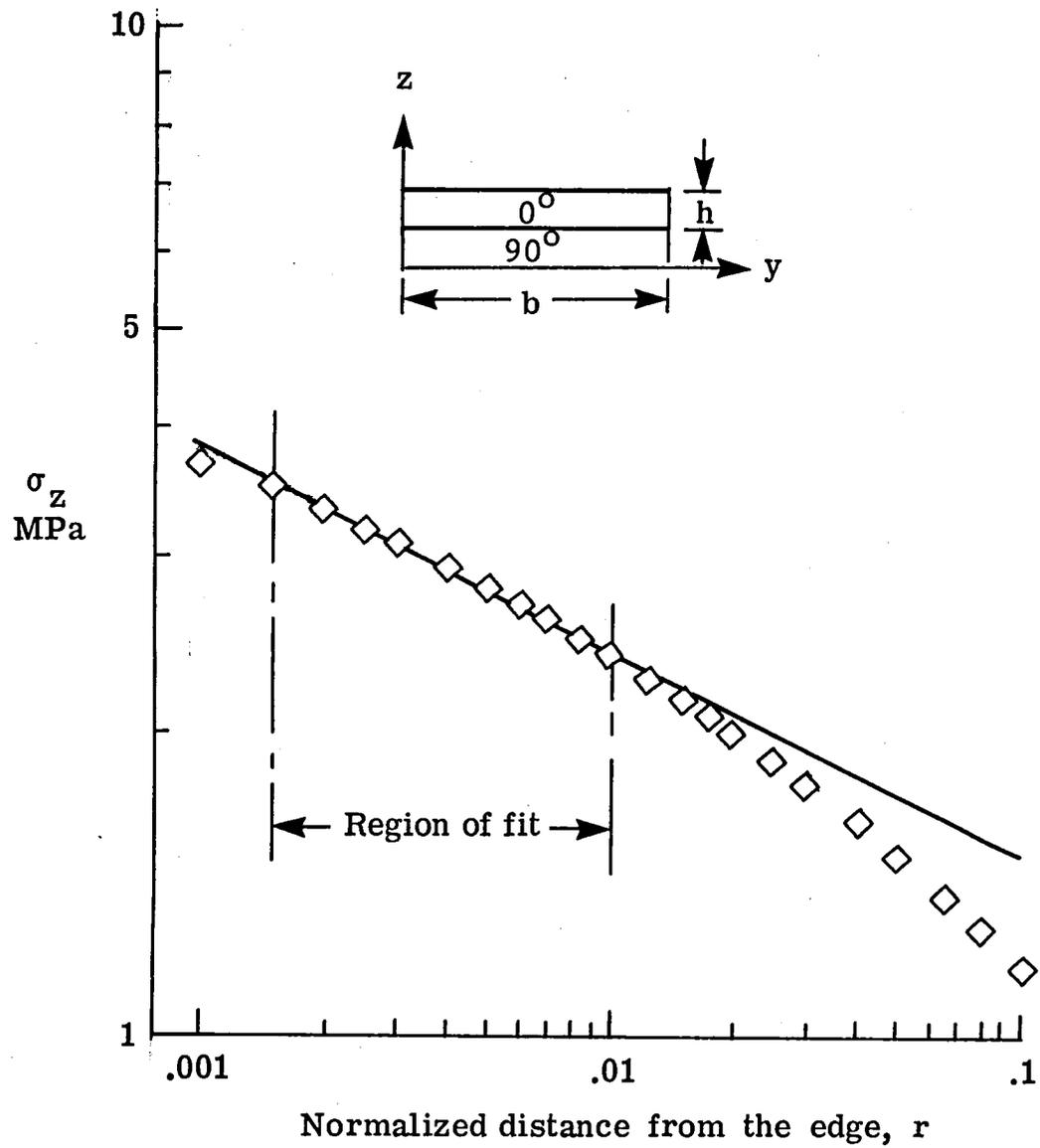
Figure 13.- Log-log plot for σ_z along the interface $(z = h)$ for a $[0/90]_s$ laminate.

1. Report No. NASA TM-81876	2. Government Accession No.	3. Recipient's Catalog No.
4. Title and Subtitle INTERLAMINAR STRESS SINGULARITIES AT A STRAIGHT FREE EDGE IN COMPOSITE LAMINATES		5. Report Date August 1980
		6. Performing Organization Code
7. Author(s) I. S. Raju and John H. Crews, Jr.		8. Performing Organization Report No.
9. Performing Organization Name and Address		10. Work Unit No. 506-53-53-01
NASA Langley Research Center Hampton, VA 23665		11. Contract or Grant No.
12. Sponsoring Agency Name and Address		13. Type of Report and Period Covered Technical Memorandum
National Aeronautics and Space Administration Washington, DC 20546		14. Sponsoring Agency Code

15. Supplementary Notes

16. Abstract

    A quasi-three-dimensional finite-element analysis was used to analyze the edge-stress problem in four-ply, composite laminates. The seven laminates that were considered belong to the laminate family $[\theta/(\theta-90)]_s$, where $0 \leq \theta \leq 90$. Systematic convergence studies were made to explore the existence of stress singularities near the free edge. The present analysis appears to confirm the existence of stress singularities at the intersection of the interface and the free edge. The power of the stress singularity was the same for all seven laminates considered.

17. Key Words (Suggested by Author(s))	18. Distribution Statement
Composite laminates Interlaminar stresses Finite elements Stress singularity	Unclassified - Unlimited Subject Category 39

19. Security Classif. (of this report)	20. Security Classif. (of this page)	21. No. of Pages	22. Price*
Unclassified	Unclassified	29	A03